

# Polyelectrolyte Complex Tubular Membranes via a Salt Dilution Induced Phase Inversion Process

Stephan Emonds, Johannes Kamp, Julian Borowec, Hannah Roth, and Matthias Wessling\*

Tubular membrane geometries are key elements of many industrial filtration applications and artificial organs. Established processes to fabricate polymeric membranes require the use of organic solvents, which are prone to be phased out due to stricter regulations. In the quest of developing solvent-free alternative fabrication processes, polyelectrolyte complex (PEC) membranes are recently discovered, offering a promising alternative. While flat sheet PEC membranes are successfully fabricated, tubular or hollow fiber geometries remain a material engineering challenge. For the first time, the organic solvent-free fabrication of PEC tubular membranes in a dry-jet wet spinning process is demonstrated. The aqueous polymer solution comprising the polyanion—poly(sodium-4-styrenesulfonate) (PSS), the polycation—poly(diallyldimethylammonium-chloride) (PDADMAC), and KBr is extruded with the water-based bore fluid through a single-orifice spinneret, passing an air-gap before immersed into an aqueous coagulation bath. The phase inversion kinetics are influenced to form a defect-free lumen separation layer through the addition of glycerol to the bore fluid. The resulting tubular membranes show reproducible nanofiltration membrane properties. They have a molecular cut-off of 320 Da, are positively charged and retain salts with a characteristic salt retention hierarchy. This promising material engineering strategy motivates to continue the quest for smaller tubular dimensions toward hollow fibers.

## 1. Introduction


The use of tubular membranes instead of flat sheet membranes has improved membrane reactors and membrane filtration processes such as microfiltration and ultrafiltration significantly in the past decades.<sup>[1–3]</sup> The tubular membrane geometry has advantages in terms of an improved fluid dynamic that does not require spacers. Therefore, the fouling potential is reduced and the cleaning process is easier.<sup>[4,5]</sup> The fabrication of tubular and hollow fiber nanofiltration composite membranes based on organic solvents and crosslinkers is still investigated and developed.<sup>[6–13]</sup> However, the use of organic solvents needs to be avoided and more benign fabrication procedures need to be focused on. Even national and international authorities such as the EU starts to limit the usage of organic solvents,<sup>[14]</sup> which are essential for the fabrication of polymeric membranes using the established nonsolvent-induced phase separation (NIPS) method. A variety of novel solvents is being investigated for the estab-

lished membrane forming polymers polyethersulfone (PES), polyvinylidene difluoride (PVDF), and polysulfone (PSF).<sup>[15–18]</sup> However, an all-aqueous based fabrication process could be highly viable in eliminating organic solvents completely.

Polyelectrolyte complexes (PECs) offer such a materials engineering platform. Polyelectrolytes are polymers with ionic functional groups covalently bound to the polymer backbone. Polyelectrolytes are soluble in water, so the use of organic solvents can be avoided. When oppositely charged polyelectrolytes are mixed in an aqueous environment, they form solid complexes by ionic interactions between polyanions and polycations. The complexation is induced due to an entropic-free energy reduction by the release of the many counterions.<sup>[19,20]</sup> The binding between polyanions and polycations in the aqueous polymer solution strongly depends on the ionic strength and can be controlled by the addition of salt, the variation of the pH and the temperature in the solution.<sup>[19,20]</sup> A high ionic strength weakens the ionic interactions between the polyelectrolytes due to the charge shielding of the ionized groups. By increasing the ionic strength, e.g., by the addition of salt, the complex formation can be suppressed and the polyelectrolyte aqueous mixture forms a

S. Emonds, J. Borowec, H. Roth, Prof. M. Wessling  
DWI – Leibniz-Institute for Interactive Materials  
Forckenbeckstraße 50, Aachen 52074, Germany  
E-mail: Manuscripts.cvt@avt.rwth-aachen.de

S. Emonds, J. Kamp, J. Borowec, H. Roth, Prof. M. Wessling  
Chemical Process Engineering AVT.CVT  
RWTH Aachen University  
Forckenbeckstraße 51, Aachen 52074, Germany

 The ORCID identification number(s) for the author(s) of this article can be found under <https://doi.org/10.1002/adem.202001401>.

© 2021 The Authors. Advanced Engineering Materials published by Wiley-VCH GmbH. This is an open access article under the terms of the Creative Commons Attribution-NonCommercial-NoDerivs License, which permits use and distribution in any medium, provided the original work is properly cited, the use is non-commercial and no modifications or adaptations are made.

DOI: 10.1002/adem.202001401

coacervate. A coacervate is a liquid–liquid two phase system with an equilibrium between the polymer rich and the polymer lean phase. At an ionic strength beyond the critical point, a one-phase homogeneous liquid solution forms. At this point, no interactions between the polyelectrolytes are present.<sup>[21]</sup> A controlled initiation of polyelectrolyte complexation enables the fabrication of solid complexes with controlled porosity. In this case, water with high ionic strength acts as a solvent and water with low ionic strength as a nonsolvent.

First investigations of polyelectrolyte complexation are reported by Jong et al. in 1930.<sup>[22]</sup> To this day, different research groups report the fabrication of biomaterials, coatings, and membranes solely or partly based on PECs.<sup>[21,23–28]</sup> Recently published solvent-free fabrication procedures of PEC membranes represent promising alternatives to established membrane fabrication methods because water is used as a solvent and nonsolvent. One method uses a combination of strong and weak polyelectrolytes.<sup>[27,29]</sup> In contrast to strong polyelectrolytes, the charge of a weak polyelectrolyte strongly depends on the pH. Therefore, the complexation can be suppressed by adjusting the pH and can be induced by a pH shift. For strong polyelectrolytes, that are desired to fabricate pH stable materials, a pH adjustment is not suitable. A high salt concentration allows the formation of a homogeneous polymer solution out of strong polyelectrolytes.<sup>[30]</sup> In fact, the fabrication of flat-sheet PEC membranes has been developed already.<sup>[21,25,26,28]</sup> The transfer of these materials' concept to tubular geometries is the next frontier in the solvent-free fabrication processes of porous membranes.

In contrast to flat-sheet membranes, the advantages of tubular and hollow fiber membranes promise a more economical and resource efficient filtration process. Although the complexation mechanism during phase inversion of cast films, tubular and hollow fiber membranes are similar, in the dry-jet wet spinning process, two coagulation fluids induce the phase separation. On the lumen side, phase separation is induced by the bore fluid, which contacts the polymer solution directly after the spinneret and shapes the tubular membrane. On the shell side, the tubular membrane contacts the coagulation bath subsequently. Furthermore, the continuous dynamic spinning process increases the complexity while offering additional opportunities for the control of the coagulation process and resulting tubular membrane properties.<sup>[31–33]</sup> During the spinning process, multiple parameters such as the composition of the bore fluid, the spinneret geometry, the flow rates of the polymer solution and bore fluid, the air gap as well as the take-up speed, have a major impact.<sup>[31,33,34]</sup> Thus, a continuous dry-jet wet spinning of polymeric tubular membranes is complex and many different process parameters need to be considered and controlled. We successfully transferred the salt dilution-induced phase separation to a tubular membrane spinning process. The resulting asymmetric tubular membranes have a dense separation nanofiltration layer and an open porous substructure.

## 2. Results and Discussion

In this work, we present the dry-jet wet spinning of PEC tubular membranes. Based on our expertise in flat-sheet membrane fabrication with the material system of our recent study,<sup>[21]</sup> we

developed appropriate spinning solution compositions and parameters that allow for the continuous fabrication of tubular membranes.

The polymer solution comprises poly(sodium 4-styrenesulfonate) (PSS) (average  $M_w \approx 1\,000\,000$ ) and poly(diallyldimethylammonium chloride) (PDADMAC) (average  $M_w \approx 400\,000$ – $500\,000$ ), water and an overcritical potassium bromide (KBr) concentration. The high KBr concentration suppresses the polyelectrolyte complexation, forming an overcritical liquid polymer solution. The polymer solution and an aqueous bore fluid are extruded through a 3D-printed single orifice spinneret (cf. **Figure 1**). The 3D-printed spinneret was manufactured as presented by Luelf et al.<sup>[35]</sup> More details about the 3D-printed spinneret are given in Experimental Section and the Supporting Information.

The extruded polymer solution and the aqueous bore fluid pass the air gap, where polyelectrolyte complexation and precipitation is initiated at the tubular lumen surface due to the contact with the aqueous bore fluid. Subsequently, it immerses in the aqueous coagulation bath, which leads to further polyelectrolyte complexation and precipitation. A porous tubular membrane forms. The corresponding solution compositions and spinning parameters are stated in the Experimental Section. By controlling all these parameters properly, PEC tubular membranes were produced continuously.

A batch of tubular membranes spun with pure water as bore solution showed nonreproducible membrane transport properties. Especially, the retention of uncharged solutes varied strongly. One sample achieved a molecular weight cut-off of 850 Da, whereas two other samples lead to MWCOs larger than 15 000 Da (cf. Table S4, Supporting Information). This shows that the continuous dry-jet wet spinning process is prone to form defects in the separation layer, when using pure water as a bore fluid.

From the conventional NIPS spinning process, it is well known that the bore fluid has a major influence on the formation of a defect-free separation layer of porous tubular and hollow fiber membranes.<sup>[32,33,36]</sup> The selection of the bore fluid affects the kinetics and the extent of nonsolvent-induced phase inversion.<sup>[34,37]</sup> Using a bore fluid with pure nonsolvent only, typically leads to the formation of a dense and smooth lumen channel surface.<sup>[38,39]</sup> In contrast, the addition of a solvent or

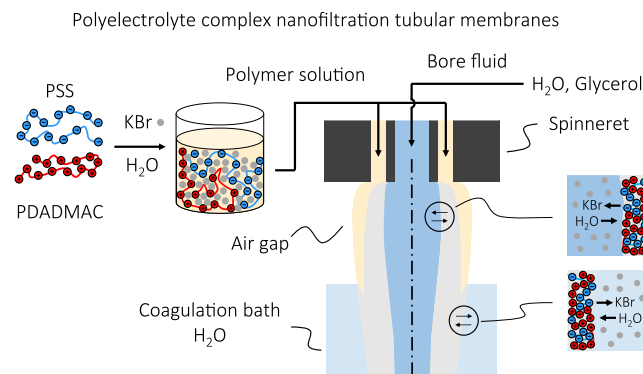


**Figure 1.** Dry-jet wet spinning of an overcritical homogeneous polyelectrolyte polymer solution forming PEC tubular membranes via salt dilution-induced phase separation.

additives such as ethylene glycol or glycerol to the bore fluid decreases the phase inversion kinetics and a rough surface layer with fewer defects forms.<sup>[33,40]</sup> Furthermore, additives in the bore fluid such as glycerol increase the fluid viscosity and minimize the collapsing of the tubular membrane.<sup>[33]</sup> The beneficial effects of increased viscosity can be used in the all aqueous phase separation spinning process using polyelectrolytes. Still, the impact on phase inversion kinetics and resulting morphology need to be investigated. Therefore, we analyzed the phase inversion kinetics using light transmittance measurements. Cast films were immersed in water and a 50 wt% water and 50 wt% glycerol mixture, while measuring the light transmittance during the phase separation, presented in **Figure 2** on the left. Field emission scanning electron microscopy (FESEM) images of the evolving membrane morphologies are given on the right of **Figure 2**. All full-scale FESEM images are provided in Figure S4 and S5, Supporting Information.

For pure water, the transmittance in the first 5 s decreases strongly. This phase inversion kinetics leads to an asymmetric membrane morphology with a dense thin surface layer and closed cells underneath, as shown in **Figure 2a,b**, right, H<sub>2</sub>O. The following open porous substructure is formed through a slight delay and a change of the composition in the film during demixing and precipitation. In contrast, for the 50 wt% water and 50 wt% glycerol mixture, a fast decrease in the first half second evolves (cf. **Figure 2**, left), forming a thicker dense surface layer compared with pure water (cf. **Figure 2**, right, H<sub>2</sub>O & glycerol (b)). Therefore, the diffusion of water in and salt ions out of the film is hindered. The resulting delay of demixing is observable in the plateau region in the transmittance (cf. **Figure 2**, left). Therefore, larger interconnected pores form in the underlying structure. The addition of glycerol to the aqueous coagulation bath forming a thicker, dense top layer thus, represents a possible way to prevent defects. As a result of these promising insights, we used the water–glycerol mixture as the bore fluid

to form a defect-free separation layer on the lumen side of the tubular membrane. Furthermore, the addition of glycerol leads to an increased viscosity of 24 mPas, stabilizing the evolving tubular membrane during spinning.

Using the bore fluid comprising glycerol resulted in stable continuous tubular membranes with a defect-free separation layer and therefore creates highly reproducible results. Later, the characterization results of the PEC tubular membranes from spinning with the aqueous bore fluid comprising 50 wt% glycerol are presented. **Figure 3** on the left shows a light microscope image of the round PEC tubular membrane.

It has an inner diameter of 4.4 mm. The lumen and shell surface are smooth and the wall thickness of around 200  $\mu\text{m}$  is constant. The tubular membrane is freestanding, has a circular lumen channel and is soft while elastic under wet conditions.

On the right of **Figure 3**, the FESEM images of the tubular membrane cross section are presented to evaluate the different morphologies in more detail. All full-scale FESEM images are shown in **Figure S8**, Supporting Information. In **Figure 3a**, the cross section shows the asymmetric morphology of the tubular membrane. It has two dense layers, on the lumen and on the shell side. In between, an open porous membrane structure is visible, whereas the pore sizes increase toward the lumen side.

The enlarged top layer section of the lumen side in **Figure 3b** shows the well-integrated dense top layer onto the porous substructure with interconnected pores (cf. **Figure 3b,c**). The morphology, in terms of thickness of the dense layer, as well as the pore structure underneath, is very similar to the morphology of the flat membrane shown in **Figure 2** (right, H<sub>2</sub>O & glycerol). This asymmetric membrane morphology typically results from delayed demixing in the phase inversion process, which was observed in the light transmittance measurements (cf. **Figure 2**, left).<sup>[40,41,42]</sup> During salt dilution, the high salt concentration gradient between the bore fluid and polymer solution leads to the complexation and precipitation of the surface layer,

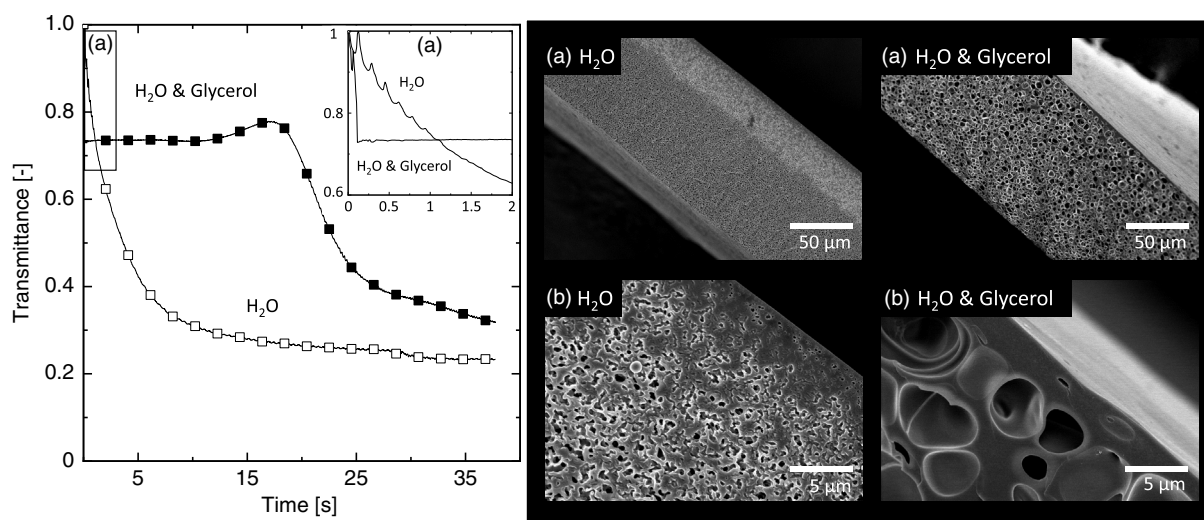


**Figure 2.** Light transmittance measurement results during phase inversion of cast films of polyelectrolyte polymer solutions immersed in the coagulation bath with pure H<sub>2</sub>O and a 50 wt% H<sub>2</sub>O and 50 wt% glycerol mixture (left); field emission scanning electron microscope images of the cross section of the evolving membranes immersed in the coagulation bath with pure H<sub>2</sub>O and a 50 wt% H<sub>2</sub>O and 50 wt% glycerol mixture (right) a) cross section, b) enlarged cross section on the lumen side.

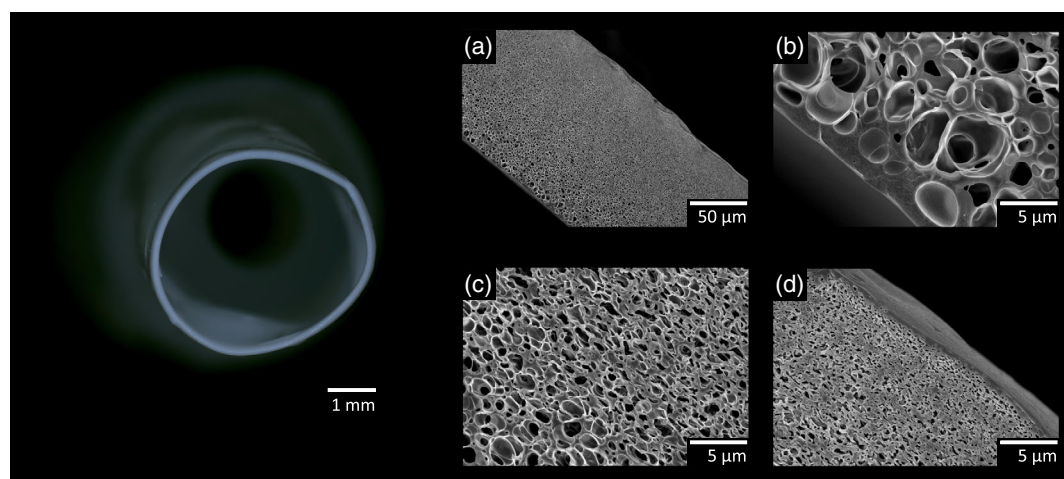


**Figure 3.** Light microscope image of the PEC tubular membrane (left); field emission scanning electron microscope images of the PEC tubular membrane (right) a) cross section, b) enlarged cross section on the lumen side, c) enlarged cross section in the middle section, and d) enlarged cross section on the shell side.

forming a dense layer. This layer hinders the salt and water exchange in the underlying regions, so larger pores form.

In comparison, Figure 3d shows the cross-sectional morphology on the shell side. The shell side structure has a thinner dense surface layer with small pores underneath. In contrast to the bore fluid comprising glycerol, the pure water coagulation bath leads to the formation of the thin dense layer with smaller open pores underneath. Even, the morphology is similar to the membranes from pure water as a coagulation media in Figure 2 (right, H<sub>2</sub>O), a direct comparison is hardly possible as the polymer concentration has already changed during phase separation toward the lumen side. Still, the influence of the two different coagulation media on the overall morphology is observable with the thicker dense layer followed by the sublayer with large pores on the lumen side, whereas on the shell side a thin dense layer followed by smaller pores in the sublayer is present (cf. Figure 3b,d).

On the one hand, the thicker dense lumen surface layer represents a high mass transport resistance, but on the other hand, it ensures a high selectivity and minimizes the potential of defect formation. A targeted variation of the glycerol concentration in the bore fluid would allow the tailoring of the membrane performance parameters and properties. Further development should focus on the phase inversion process on the shell surface. The addition of salts, solvents or additives to the coagulation bath and controlling the humidity in the air gap by a chimney as well as the air gap length deliver opportunities to create an open porous shell side morphology.

Mechanical properties of the tubular membranes require support when operated under elevated pressures. Thus, more research needs to focus on the mechanical stability improvement of the PEC material. Further membrane properties such as water contact angle and Young's modulus are provided in Figure S9 and S10, Supporting Information. For the filtration experiments, we used a tubular ceramic support to stabilize the soft freestanding PEC tubular membrane. The filtration of uncharged solutes reveals a molecular weight cut-off of  $320 \pm 0$  Da, which is a typical value for tight nanofiltration membranes.

In Figure 4, the results of single salt retention experiments with four different salts show the salt retention hierarchy of the tubular membrane.

Each data point represents the results of two membrane samples. The highest retention of 92% is achieved for MgCl<sub>2</sub> and followed by 70% for MgSO<sub>4</sub>, 54% for NaCl, and 27% for Na<sub>2</sub>SO<sub>4</sub>. The results of zeta potential measurements in Figure 5 shows a positive surface charge.

The accumulation of the polycation PDADMAC at the membrane surface, resulting in a positive zeta potential, was already discussed in our previous work in the formation of flat sheet membranes.<sup>[21]</sup> The positive surface charge supports the charge dominated retention behavior. The bivalent cation Mg<sup>2+</sup> is repelled at the membrane surface, which leads to the highest

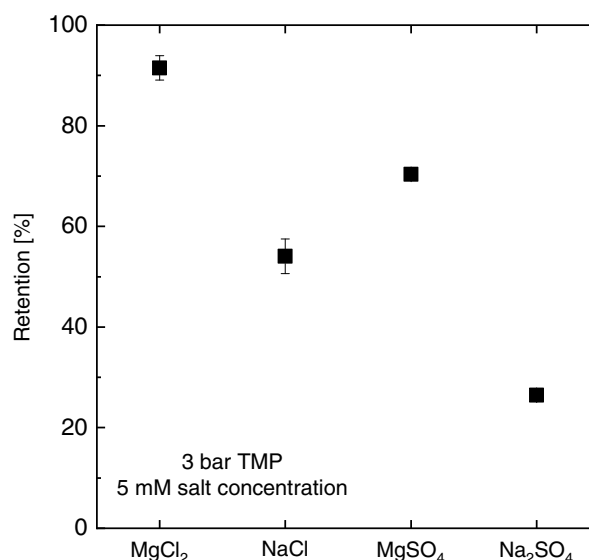


**Figure 4.** Salt retention hierarchy of the PEC tubular membrane. The salt retentions were measured with single salts at 3 bar transmembrane pressure (TMP) and 5 mM salt concentration.



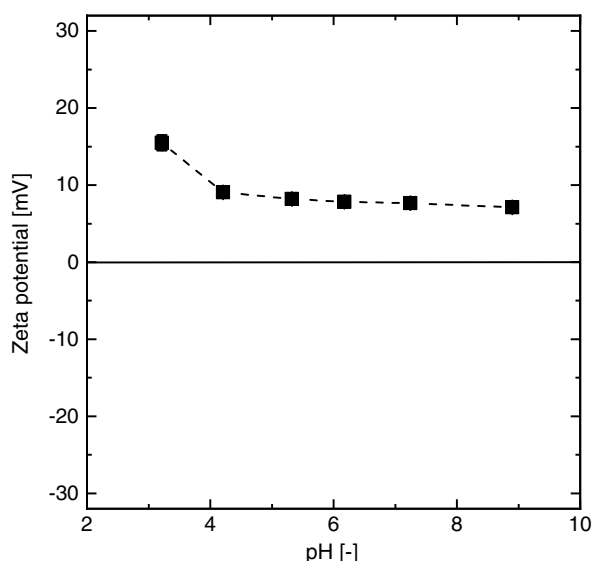


**Figure 5.** Zeta potential of the PEC tubular membrane lumen surface as a function of pH.

retention. In contrast, the lowest retention was measured for  $\text{Na}_2\text{SO}_4$  with the negative-charged bivalent anion  $\text{SO}_4^{2-}$ . This salt retention hierarchy proves a positive-fixed charge density in the membrane and therefore a Donnan exclusion dominated retention behavior.<sup>[43]</sup> A more detailed discussion on ion rejections requires suitable models, including the fixed charge distribution over the effective membrane thickness.<sup>[44]</sup>

A pure water permeance of  $0.1 \pm 0$  LMH/bar was measured. We attribute the low permeance to: a) the two dense lumen and shell layers, b) the partly closed cell structure of the porous wall, and c) the compaction of the porous substructure. The molecular weight cut-off and high salt retentions agree with the morphology and prove nanofiltration properties.

Overall, the presented spinning process results in membrane morphologies and selectivities similar to membranes fabricated via the established NIPS using organic solvents. In contrast to the common nanofiltration membrane fabrication processes, the presented method only applies one-phase inversion step without organic solvents and additional crosslinking. Moreover, no harmful components, such as trimesoyl chloride (TMC), glutaraldehyde (GA) or *n*-methyl-2-pyrrolidone (NMP) that are typically used for crosslinking or as an organic solvent, are required.

### 3. Conclusion

The organic solvent-free fabrication of freestanding PEC tubular membranes via a dry-jet wet spinning was successfully demonstrated in this work. The polymer solution comprises the polyanion PSS and the polycation PDADMAC, which are dissolved in an aqueous solution with an overcritical KBr concentration. The high KBr concentration suppresses the polyelectrolyte complexation. For the first time, the salt dilution-induced phase inversion was applied in the dry-jet wet spinning process forming tubular membranes. Identifying appropriate spinning parameters and solution compositions resulted in highly

reproducible membrane properties. Especially, the addition of glycerol to the bore fluid leads to an enhanced viscosity, preventing the tubular membrane from collapsing. We showed that a 50:50 wt% water–glycerol mixture leads to a delayed demixing, forming a defect-free dense separation layer on the lumen side. The tubular membranes have a porous asymmetric structure with dense lumen and shell surface layers, which can be tuned through the coagulation media in the bore fluid and coagulation bath. Filtration experiments of uncharged solutes reveal a low molecular weight cut-off of 320 Da, which proves that the tubular membranes have nanofiltration properties. The zeta potential and the salt retention hierarchy indicate a positive membrane surface charge leading to a high retention for  $\text{MgCl}_2$  of 92% due to Donnan repulsion. The low pure water permeance of 0.1 LMH/bar is attributed to the two dense layers and membrane compaction. By improving the mechanical strength and controlling the phase inversion in upcoming studies, an increased permeance is anticipated and the use of a support structure is avoided. In contrast to established nanofiltration fabrication processes, requiring multiple consecutive preparation steps, the presented platform is a unique single-step process based on environmentally benign processing liquids. This new all-aqueous phase inversion method gives a promising perspective for the development of alternative sustainable polymeric tubular and hollow fiber membrane fabrication processes, which are also in compliance with upcoming regulations on restricting the use of harmful solvents.

### 4. Experimental Section

**Materials:** Commercial polyelectrolytes PSS (average  $M_w \approx 1\,000\,000$  powder) and PDADMAC (average  $M_w \approx 400\,000$ – $500\,000$  (high molecular weight), 20 wt% in  $\text{H}_2\text{O}$ ) were purchased from Sigma Aldrich. Potassium bromide (KBr) was supplied by Alfa Aesar and glycerol with a purity above 99% by Carl Roth. Polyethylene glycols (PEG) with different molecular weights (200, 400, 600, 1000, 1500, 6000, and  $35\,000\text{ g mol}^{-1}$ ) and magnesium chloride ( $\text{MgCl}_2$ ), sodium chloride ( $\text{NaCl}$ ), magnesium sulfate ( $\text{MgSO}_4$ ), and sodium sulfate ( $\text{Na}_2\text{SO}_4$ ) were supplied by Sigma Aldrich.

**Membrane Fabrication:** A polymer solution comprising 14 wt% PSS, 11 wt% PDADMAC, 15 wt% KBr, and 60 wt%  $\text{H}_2\text{O}$ , and an aqueous solution with 50 wt% glycerol was used as the bore fluid. The air gap was 3.5 cm. During spinning, the flow rate of the polymer solution was 3.6 and 60  $\text{mL min}^{-1}$  of the bore fluid. The bore needle of the 3D-printed spinneret had a diameter of 2.5 mm, the polymer outlet had an inner diameter of 3.5 mm and an outer diameter of 5.0 mm. The 3D-printed spinneret was manufactured with an OBJET Eden260V 3D Printing System by Stratasys Ltd., producing parts via the poly-jet printing principle. More details about the spinneret are given in the Supporting Information.

**Light Transmittance Measurements:** The polyelectrolyte polymer solution was cast as a 200  $\mu\text{m}$  thick flat film on a glass plate and immersed horizontally in the light transmittance measuring cell. The light source was directed to the glass plate with the film and a detector behind the glass plate records the transmittance signal.

**Membrane Morphology Characterization:** The membrane morphology was analyzed with FESEM. Images of the tubular membrane cross-section were taken with FESEM Hitachi S4800 device.

**Zeta Potential:** Zeta potential was measured with SurPASS electrokinetic analyzer (Anton Paar, Austria) device at different pH values by an automated titration unit.

**Membrane Module Fabrication:** A tubular membrane was inserted in the lumen channel of a ceramic membrane tube, which functions as a mechanical support. The ceramic membrane tube was supplied by Atec Innovations GmbH. It was made from  $\text{Al}_2\text{O}_3$  and had a lumen diameter

of 6 mm and 0.8  $\mu\text{m}$  pore size. More details about the membrane module are given in the Supporting Information.

**Pure Water Permeance:** The pure water permeance was measured dead-end at 3 bar TMP.

**Molecular Weight Cut-Off:** The molecular weight cut-off was determined by cross flow filtration experiments. The aqueous feed solution contained 1 g L<sup>-1</sup> of each different-sized PEG (200, 400, 1500, 6000, 10 000, 35 000 g mol<sup>-1</sup>). Retentate and permeate concentrations were analyzed with size-exclusion chromatography (SEC) using an Agilent 1200 system.

**Salt Retention:** Cross flow filtration was conducted in single salt filtration experiments with MgCl<sub>2</sub>, NaCl, MgSO<sub>4</sub> and Na<sub>2</sub>SO<sub>4</sub>. About 5 mM of each salt was used and the filtration was conducted inside-out at 3 bar TMP. The conductivities of the retentate and permeate were measured with a conductivity meter (SevenCompact pH/Cond S213, Mettler Toledo).

## Supporting Information

Supporting Information is available from the Wiley Online Library or from the author.

## Acknowledgements

S.E. and J.K. contributed equally to this work. The authors thank Deniz Rall for providing the technical drawing and development of the 3D printed spinneret. The authors thank Karin Faensen for the high-quality SEM images. This work was conducted in part at the Center for Chemical Polymer Technology CPT, which is supported by the EU and the Federal State of North Rhine-Westphalia (grant no. EFRE 30 00 883 02). M.W. acknowledges DFG funding through the Gottfried Wilhelm Leibniz Prize 2019.

Open access funding enabled and organized by Projekt DEAL.

## Conflict of Interest

The authors declare no conflict of interest.

## Data Availability Statement

Research data are not shared.

## Keywords

all aqueous phase separation processes, dry-jet wet spinning, nanofiltration membranes, polyelectrolyte complex membranes

Received: November 21, 2020

Revised: January 21, 2021

Published online:

- [1] P. Krzeminski, J. A. Gil, A. F. van Nieuwenhuijzen, J. H. van der Graaf, J. B. van Lier, *Desalin. Water Treat.* **2012**, 42, 100.
- [2] C. Y. Feng, K. C. Khulbe, T. Matsuura, A. F. Ismail, *Sep. Purif. Technol.* **2013**, 111, 43.
- [3] D. M. Warsinger, S. Chakraborty, E. W. Tow, M. H. Plumlee, C. Bellona, S. Loutatidou, L. Karimi, A. M. Mikelonis, A. Achilli, A. Ghassemi, L. P. Padhye, S. A. Snyder, S. Curcio, C. Vecitis, H. A. Arafat, J. H. Lienhard, *Prog. Polym. Sci.* **2016**, 81, 209.
- [4] B. Zeki, *Food Process Engineering and Technology, Food Science and Technology* (Ed: B. Zeki), Academic Press, San Diego **2009**, pp. 233–257.

- [5] R. W. Baker, *Membrane Technology and Applications*, 3rd ed., John Wiley & Sons, Chichester, West Sussex and Hoboken **2012**.
- [6] J. Y. Chong, R. Wang, *J. Memb. Sci.* **2019**, 587, 117161.
- [7] J. Kamp, S. Emonds, M. Wessling, *J. Memb. Sci.* **2020**, 118851.
- [8] D. Menne, J. Kamp, J. Erik Wong, M. Wessling, *J. Memb. Sci.* **2016**, 499, 396.
- [9] H. Roth, T. Luelf, A. Koppelman, M. Abel, M. Wessling, *J. Memb. Sci.* **2018**, 554, 48.
- [10] E. Virga, J. de Grooth, K. Žvab, W. M. de Vos, *Materials* **2019**, 1, 2230.
- [11] E. te Brinke, I. Achterhuis, D. M. Reurink, J. de Grooth, W. M. de Vos, *ACS Appl. Polym. Mater.* **2019**, 2, 715.
- [12] J. Gao, K. Y. Wang, T.-S. Chung, *J. Memb. Sci.* **2020**, 603, 118022.
- [13] S. Emonds, H. Roth, M. Wessling, *J. Memb. Sci.* **2020**, 612, 118325.
- [14] D. Bourguignon, *EU Policy and Legislation on Chemicals: Overview, with a Focus on REACH : In-Depth Analysis*, European Parliament, Brussels **2016**.
- [15] T. Marino, F. Galiano, S. Simone, A. Figoli, *Environ. Sci. Pollut. Res.* **2019**, 29, 14774.
- [16] X. Dong, A. Al-Jumaily, I. C. Escobar, *Membranes* **2018**, 8, 2.
- [17] T. Marino, F. Galiano, A. Molino, A. Figoli, *J. Memb. Sci.* **2019**, 580.
- [18] H. H. Wang, J. T. Jung, J. F. Kim, S. Kim, E. Drioli, Y. M. Lee, *J. Memb. Sci.* **2019**, 574, 44.
- [19] A. S. Michaels, *Ind. Eng. Chem.* **1965**, 57, 32.
- [20] J. Fu, J. B. Schlenoff, *J. Am. Chem. Soc.* **2016**, 138, 980.
- [21] J. Kamp, S. Emonds, J. Borowec, M. A. Restrepo Toro, M. Wessling, *J. Memb. Sci.* **2021**, 618, 118632.
- [22] H. G. B. Jong, H. R. Kruyt, *Kolloid-Z.* **1930**, 50, 39.
- [23] F. J. Arias, V. Reboto, S. Martín, I. López, J. C. Rodríguez-Cabello, *Biotechnol. Lett.* **2006**, 28, 687.
- [24] R. J. Stewart, C. S. Wang, H. Shao, *Adv. Colloid Interface Sci.* **2011**, 167, 85.
- [25] K. D. Kelly, J. B. Schlenoff, *ACS Appl. Mater. Interfaces* **2015**, 7, 13980.
- [26] K. Sadman, D. E. Delgado, Y. Won, Q. Wang, K. A. Gray, K. R. Shull, *ACS Appl. Mater. Interfaces* **2019**, 11, 16018.
- [27] J. D. Willott, W. M. Nielsen, W. M. de Vos, *ACS Appl. Polym. Mater.* **2020**, 2, 659.
- [28] E. N. Durmaz, M. I. Baig, J. D. Willott, W. M. de Vos, *ACS Appl. Polym. Mater.* **2020**, 2, 2612.
- [29] M. I. Baig, E. N. Durmaz, J. D. Willott, W. M. Vos, *Adv. Funct. Mater.* **2019**, 30, 1907344.
- [30] Q. Wang, J. B. Schlenoff, *Macromolecules* **2014**, 47, 3108.
- [31] S. A. McKelvey, D. T. Clausi, W. J. Koros, *J. Memb. Sci.* **1997**, 124, 223.
- [32] S. Bonyadi, T. S. Chung, W. B. Krantz, *J. Memb. Sci.* **2007**, 299, 200.
- [33] A. L. Ahmad, T. A. Otitoju, B. S. Ooi, *J. Ind. Eng. Chem.* **2019**, 70, 35.
- [34] N. L. Le, S. P. Nunes, *J. Memb. Sci.* **2017**, 533, 171.
- [35] T. Luelf, D. Rall, D. Wypsek, M. Wiese, T. Femmer, C. Bremer, J. U. Michaelis, M. Wessling, *J. Memb. Sci.* **2018**, 555, 7.
- [36] N. Noor, J. Koll, N. Scharnagl, C. Abetz, V. Abetz, *Membranes* **2018**, 8, 3.
- [37] N. L. Le, B. A. Pulido, S. P. Nunes, *Ind. Eng. Chem. Res.* **2019**, 58, 22343.
- [38] Y. Bang, M. Obaid, M. Jang, J. Lee, J. Lim, I. S. Kim, *Chemosphere* **2020**, 259, 127467.
- [39] Y. Liu, G. Koops, H. Strathmann, *J. Memb. Sci.* **2003**, 223, 187.
- [40] J. A. van't Hof, A. J. Reuvers, R. M. Boom, H. Rolevink, C. A. Smolders, *J. Memb. Sci.* **1992**, 70, 17.
- [41] P. van de Witte, P. J. Dijkstra, J. van den Berg, J. Feijen, *J. Memb. Sci.* **1996**, 117, 1.
- [42] C. A. Smolders, A. J. Reuvers, R. M. Boom, I. M. Wienk, *J. Memb. Sci.* **1992**, 73, 259.
- [43] A. Yaroshchuk, *Sep. Purif. Technol.* **2001**, 22–23, 143.
- [44] E. Evdochenko, J. Kamp, R. Femmer, Y. Xu, V. Nikonenko, M. Wessling, *J. Memb. Sci.* **2020**, 611, 118045.